Ahmed H. Zewail

Femtosecond Reaction Dynamics

Elementary Processes, from Isolated to Solvated Reactions

Abstract

The field of femtochemistry is reviewed with particular focus on femtosecond reaction dynamics, from isolated to solvated reactions. As an example, the nuclear motion of a two-atom system is examined in the gas phase/molecular beam, in the presence of one (or few) solvent atoms, and in solvent cages of clusters and at high-pressure phases. We conclude by discussing future directions relating to molecular control and to the development of ultrafast diffraction.

I. Introduction

This article is the outcome of an overview lecture presented at the Royal Netherlands Academy of Arts and Sciences as part of a conference organized by Professor Dr. Douwe A. Wiersma (May 17-19, 1993). The meeting, which was superbly organized, was crafted to focus on femtosecond reaction dynamics, covering studies from the isolated-system limit to the condensed phase. The following is the contribution of research from the California Institute of Technology. Personally, I am grateful for the warm and sincere reception by colleagues at the Conference on the occasion of the awarding of the 1993 Wolf Prize in Chemistry (for this field). I wish to thank Professor Wiersma for his generous and kind efforts, and Professor John van der Waals for his thoughtful introduction and presentation of the Royal Academy Medal.

The field of 'molecular reaction dynamics' (Levine, 1987) is concerned with the understanding of chemical reactivity of *isolated* (single, full- or half-collision) systems at the molecular level. In such systems, the motion of atoms during the breaking and making of bonds involves several dynamical phenomena. Fundamentally, there are three types of ultrafast dynamics common to all chemical reactions: (1) the process of intramolecular vibrational (and rotational) energy redistribution (IVR); (2) the reactants-to-products microcanonical reaction rates, state-resolved; and (3) the dynamics of the transition states and their structures. Over the past 15 years, much progress has been made in observing and studying these processes in real-time. For a recent review, the reader is referred to Khundkar, 1990 and Zewail (1993 & 1994).

Since atoms and molecules have typical velocities on the order of 1 km/s, the elementary dynamics of transition-state structures at a resolution of angstroms are on the femtosecond (fs) time scale. This classical estimate of the femtosecond time scale for nuclear motion is also evident from transition-state theory of reaction rates:

$$k_{reaction} = (kT/h)(Q^{\ddagger}/Q_r)\, e^{-E_a/kT}$$
$$\equiv (kT/h)\, K^{\ddagger}. \tag{1}$$

In the above expression, Q_r is the product of partition functions for the reactants, and $Q^{\ddagger}$ is that of the activated complex (less the one of the reaction coordinate). $K^{\ddagger}$ is the equilibrium constant between the reactants and the activated complexes. The upper limit of kT/h is about 10^{13} sec^{-1}; this is the 'rate' at which the nuclei are expected to change their position. Thus, with sufficient time resolution, the transition-state structures can be 'frozen out.' Quantum mechanically, this picture of localization is also valid, as with fs pulses the de Broglie wavelength of a chemical system is sub-angstrom, a key feature in the studies of the

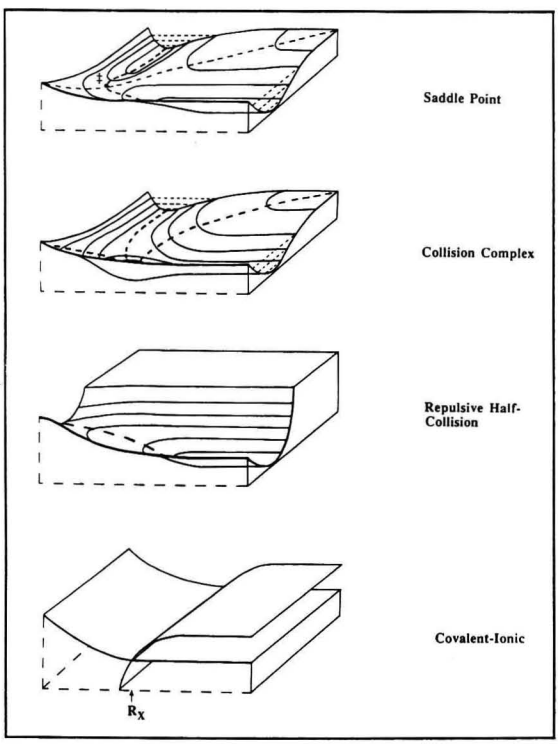

Fig. 1. Some generic potentials describing nuclear motions for different types of reactions. Drawn by Dr. M. Gruebele.

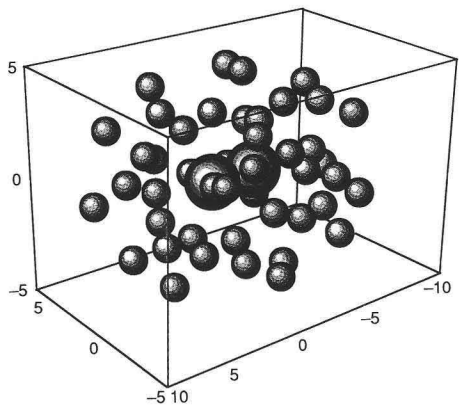

Fig. 2. Molecular dynamics simulations of the solvation structure in clusters; in this case, for iodine in argon. The atomic size is not to scale exactly (changed for better visualization).

evolution of chemical reactions in real-time. Femtochemistry (for reviews, see Zewail, 1988; 1991; 1993; 1994) is concerned with the very act of chemical transformation: the process of breaking one chemical bond and making another.

The scope of this research has spanned applications in the gas phase/ molecular beams, in clusters, on surfaces, and at the interface to the condensed

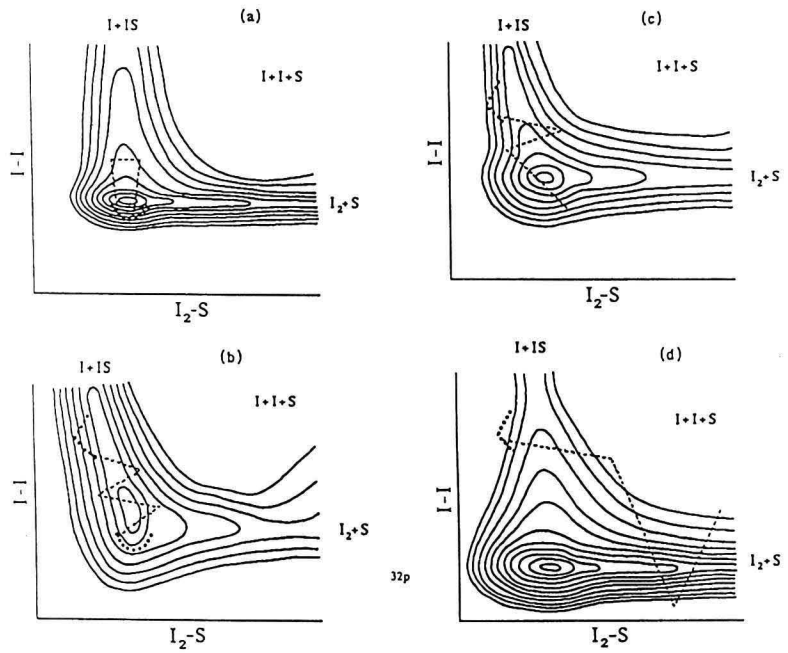

Fig. 3. Some global potentials describing the solvent-solute coordinate and the chemical I-I coordinate. [P.S. Dardi and J.S. Dahler, *J. Chem. Phys.* **98**, 363, (1993)].

phase. These applications were exemplified in the recent conference on femtochemistry in Berlin (Appendix I). The range of reactions studied includes two classes: (1) unimolecular (half-collision); and (2) bimolecular (full-collision) reactions. Fig. 1 gives some generic potentials describing the motions in these classes of reactions studied by Femtosecond Transition-state Spectroscopy (FTS). Specifically, they include: dissociation, isomerization, barrier crossing (saddle-point), intermediates of collision-complexes (potential well), electron

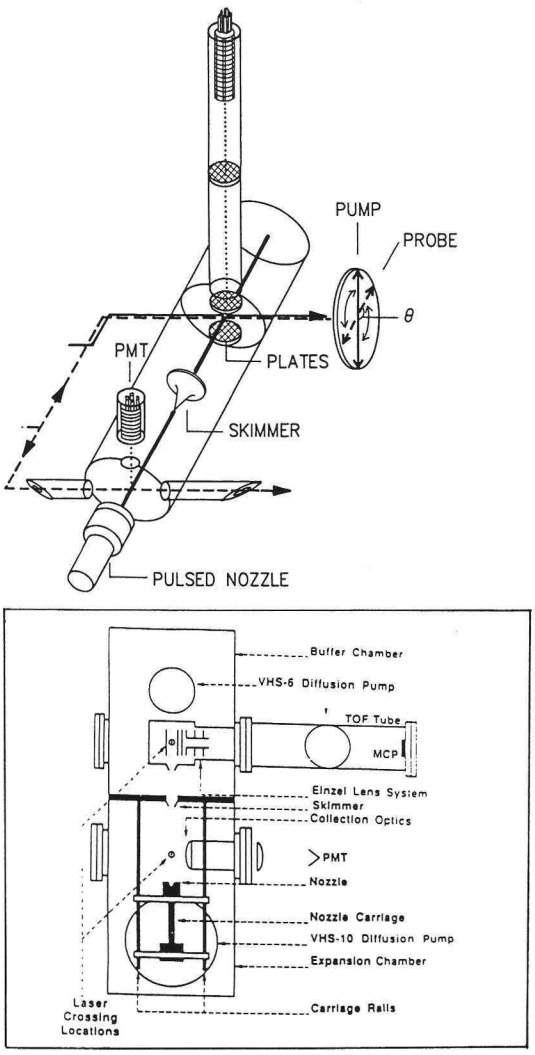

Fig. 4. (Top) Molecular beam apparatus with time-of-flight mass-spectrometer and with a laser-induced fluorescence arrangement. (Bottom) A schematic with details of another similar, but larger, beam apparatus.

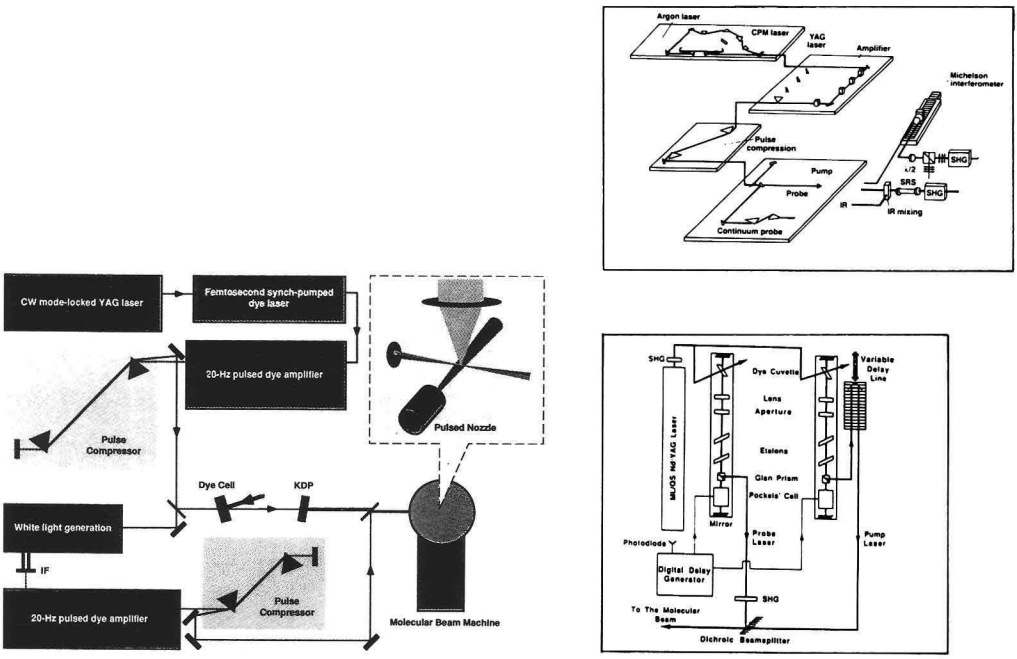

Fig. 5. Three laser systems used in these studies. (Top right) the CPM laser/amplifier system; (Bottom right) a mode-locked Q-switched Nd : YAG system with two dye lasers pumped in synchrony; (Left) A CW mode-locked YAG system with a synch-pumped dye laser, together with two amplifiers and pulse continuum generation and compression arrangements.

and proton transfers, etc. Elsewhere, these studies have been reviewed by Khundkar (1990), Porter (1992), Beddard (1993), Dantus (1991), and Zewail (1988, 1989, 1991, 1992, 1993, 1994).

Here, we wish to examine the simplest elementary reaction of two atoms in isolation and in a controlled solvent environment, developing both the concepts and the methodology. The system is that of molecular iodine and iodine with *one*, *few*, or *shells* of solvent (He, Ne, Ar, Xe) cages (Fig. 2). This systematic study allows us to examine the dynamics of elementary reactions on ultrashort time scales, 'before' and 'during' the solvent motion. Accordingly, in analogy with the description given in Fig. 1, we can now examine the trajectory of the motion, including the solvent-solute coordinate as part of the global potential (Fig. 3). The experimental approach utilizes the FTS methodology with molecular beams (or high pressure cells) (Fig. 4), along with the now standard methods of detection: laser-induced fluorescence (LIF) and mass-spectrometry. The three laser systems used are shown in Fig. 5.

II. The Potential of Free-Solute Motion

When iodine is excited with a femtosecond pulse, a wave packet is formed with the nuclei, at a given internuclear distance, localized to $\sim$0.1-0.2 Å. Fig. 6 shows

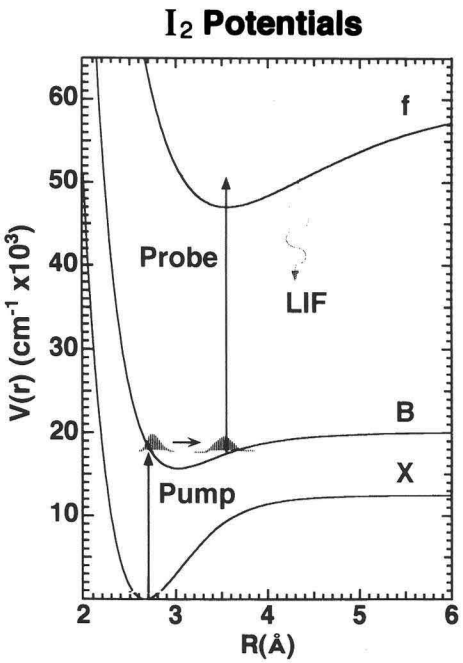

Fig. 6. The potentials for iodine, together with a typical scheme for wave packet preparation and probing [from Yan, 1992].

the wave packet preparation on the bound B-state and the probing by laser-induced fluorescence. We can also prepare wave packets above dissociation (to I + I* atoms) on the B-state potential, as well as on the A-state (not shown) to yield I + I ground-state atoms. Before considering the solvation of iodine, it is useful to show how we can deduce the potential from the femtosecond experiments (Gruebele, 1993).

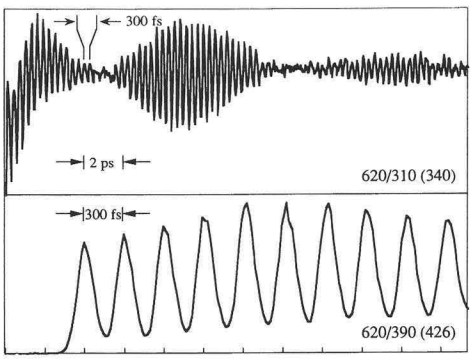

Fig. 7. The wave packet motion in iodine excited to the B-state at 620 nm, observed by LIF [R.M. Bowman, M. Dantus, and A.H. Zewail, *Chem. Phys. Lett.* **161**, 297 (1989); see also Gruebele, 1993].

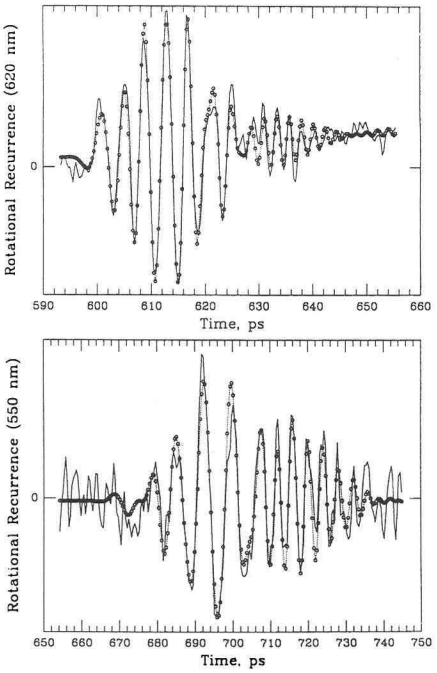

Fig. 8. The rotational recurrences observed for iodine [M. Dantus, R.M. Bowman, and A.H. Zewail, *Nature* **343**, 737 (1990); see also Gruebele, 1993].

The wave packet dynamics of *vibrational* and *rotational* motions show separate time scales corresponding to *scalar* and *vector* dependencies in the time evolution. In Figs. 7 and 8, the vibrational (femtosecond) and rotational (subnanosecond) transients are shown, and in Fig. 9 the influence of the initial temperature (beam versus cell) is displayed. From these results, one can invert the data, using, e.g., the RKR method, and obtain the potential. Experimentally, the initial position of the wave packet and the translation energy are varied by changing the total energy. In Fig. 10, three examples of wave packets, bound, dissociative, or quasi-bound, are shown and will be part of the studies of solvation discussed below. This coherent motion of a wave packet in reactive and nonreactive systems (Zewail, 1993) has become general to many systems. In solutions and clusters, such transients provide the nature of the dynamics, particularly at the early times, significant to the elementary processes.[1,2]

[1] In solutions, see the work of S. Ruhman (I_3^-), G. Fleming and N. Scherer (I_2), R. Hochstrasser (HgI_2), P. Barbara (I_2^-) in this proceeding.
[2] In clusters, see the work of C. Lineberger [$I_2^-/(CO_2)_n$], A.W. Castleman, Jr. $(NH_3)_n$, L. Wöste (Na_3), and our group (I_2/Ar_n): Papanikolas, 1992; Wei, 1992; Schreiber, 1992; and Potter, 1992; Liu, 1993. For the work of G. Gerber (Na_2, Na_3), see this proceeding and Baumert, 1992.

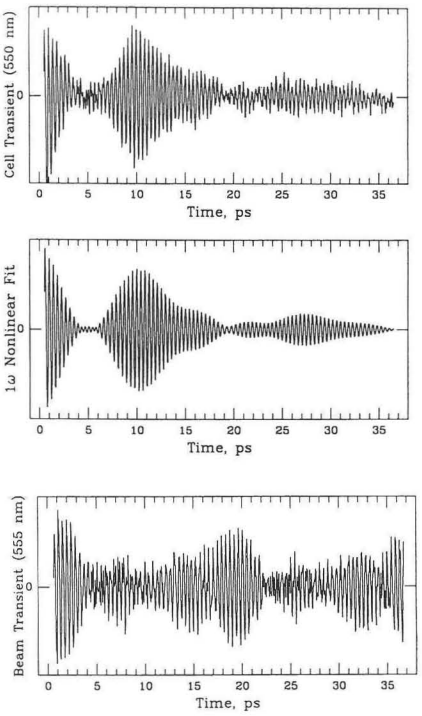

Fig. 9. Wave packet dynamics of iodine observed in a molecular beam and in a cell. The middle transient is a theoretical simulation of the top transient [Gruebele, 1993].

III. The One (and Few) Solvent-Atom Case

The simplest case for solvation is that of a one-rare gas atom attached to iodine by van der Waals forces. This complex can be made in a molecular beam and its identification and structure can be obtained from the spectroscopy. The structure of, e.g., the iodine/neon system is sketched in Fig. 11. Here, we employ an ultrafast pulse to excite the I_2 vibration (quantum number v_i') in the $I_2 \cdot Ne_n$ complex and subsequently detect the nascent I_2 in $v_{f'}$ (Fig. 12). The state-to-state dynamics can then be probed directly (Fig. 13), and the v_i' dependence of the microcanonical rates can be determined (Fig. 14). These rates allow us to describe the dynamics along the second potential coordinate, namely the intermolecular solute-solvent motion.

Designating the iodine nuclear motion by the coordinate r and the iodine-rare gas by R (Fig. 12), then the Hamiltonian can be written as follows:

$$U(r, R) = U(r_0, R) + V(r, R), \tag{2}$$

where r_0 designates the equilibrium value. The rate for the rare gas atom

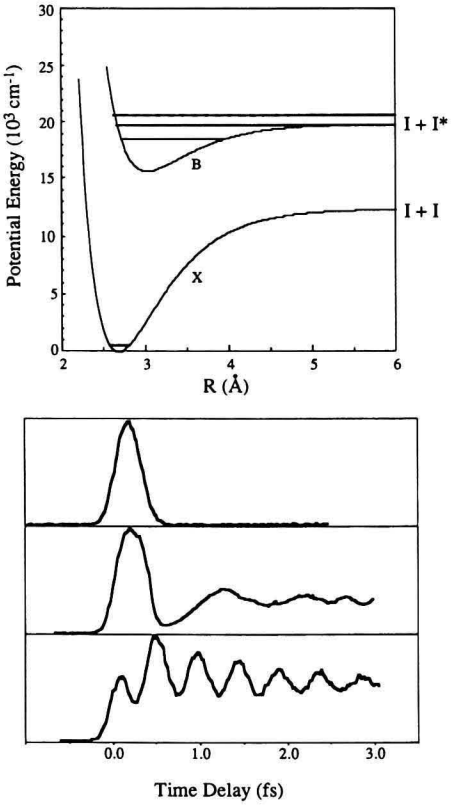

Fig. 10. Wave packet dynamics (bottom) of iodine at three energies (top); below, at, and above dissociation to I + I*.

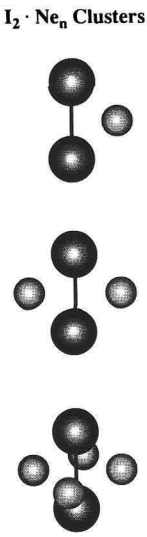

Fig. 11. View of the structures of $I_2 \cdot Ne_n$ with $n = 1, 2, 4$.

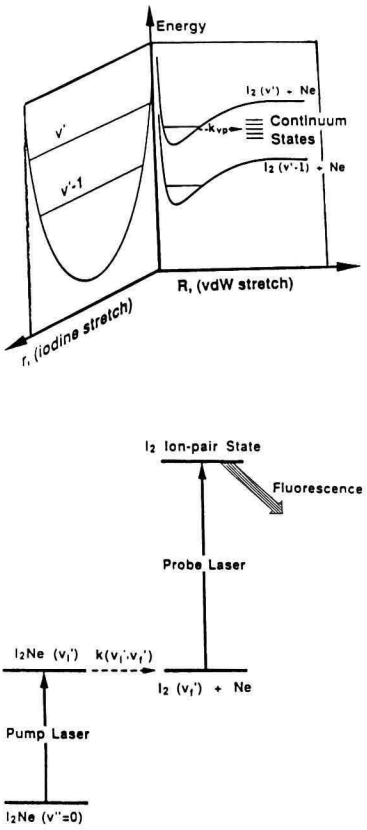

Fig. 12. (Top) The potential of I_2Ne along the intra- and intermolecular coordinates. (Bottom) The pump (reactant)-probe (product) scheme used for probing the state-to-state rates [Gutmann, 1992; Gutmann, 1992].

'evaporation' (predissociation) can be written in a simple form using a Fermi-Golden rule expression:

$$\tau^{-1} \equiv k(v_i', v_f') = \pi |\langle v_i' l' | \, V \, | v_f' \varepsilon' \rangle|^2$$
$$\equiv \pi |\langle v_i' | \, (r - r_0) \, | v_f' \rangle|^2 \, |\langle l' | \, (\partial U / \partial Q)_0 \, | \varepsilon' \rangle|^2. \tag{3}$$

Beswick and Jortner (Beswick, 1981) have shown that the first matrix element describes the v_i' dependence of the intramolecular part, and the second matrix element describes the intermolecular effect (l' is the quantum number of the vdW coordinate and ε' describes the translational continuum). A model potential and geometry can now be invoked to obtain the rates. Instead, we shall use a recent simplified model which makes it straightforward to deduce characteristic of the intermolecular potential at short distances. In this Landau-Teller-Nikitin theory, the half-collision predissociation problem is transferred to the reverse rare gas atom plus iodine full collision (Willberg, 1993). Accordingly, the rates are given

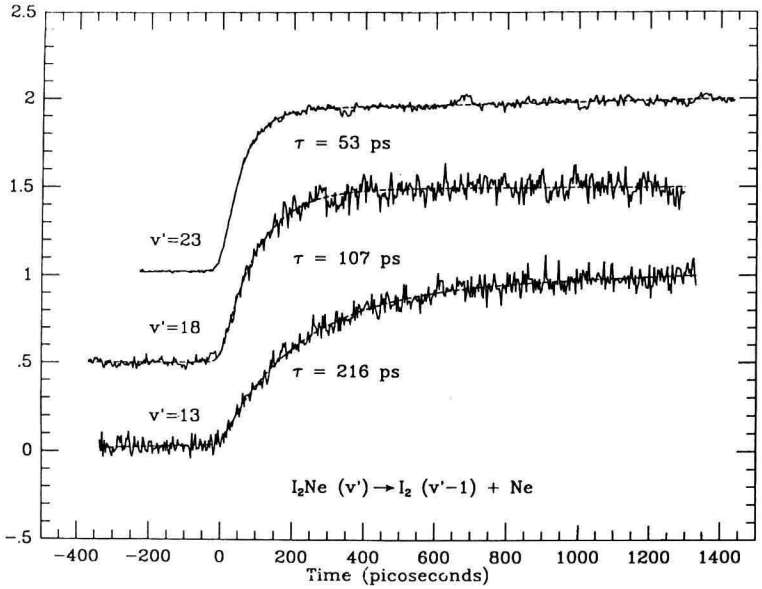

Fig. 13. Typical transients for $I_2 \cdot Ne$, following the scheme outlined in Fig. (12) [Gutmann, 1992; Gutmann, 1992].

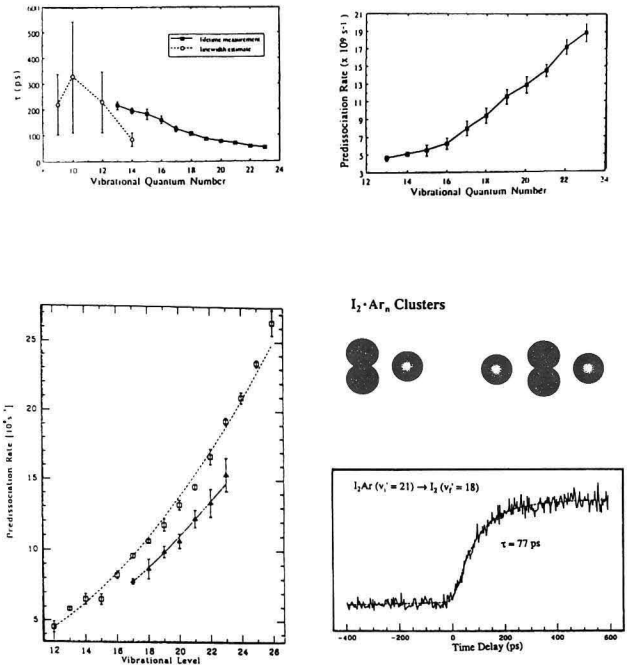

Fig. 14. The dependence of the resonance lifetime and state-to-state rates on the initial vibrational quantum number v_i'. (Top) for I_2Ne; (Bottom) left is for I_2He (Solid curve; real-time data and dashed curve is linewith data), and (Bottom) right is for $I_2 \cdot Ar$ [Gutmann, 1992; Gutmann, 1992].

by the dependence of the translational (inter) to vibrational (intra) coupling on (i) the amplitude of the vibrational motion of the iodine and (ii) the Franck-Condon factor between translational functions of a free-free transition. It is straightforward to show that (Willberg, 1993):

$$k = cv_i' e^{\gamma v_i'}, \tag{4}$$

with a highly nonlinear v_i' dependence (Fig. 14). Now γ defines the nature of the repulsive potential (exponential) and is directly related to α, the length parameter of the potential. Such treatment for iodine solvated with He, Ne, or Ar, together with real-time studies of the rates, can be found in Gutmann, 1992. The potential parameter α is typically 1.2 $Å^{-1}$ indicating a length approach of ~ 0.8 Å.

For larger number of rare gas atoms, the rates change dramatically as shown

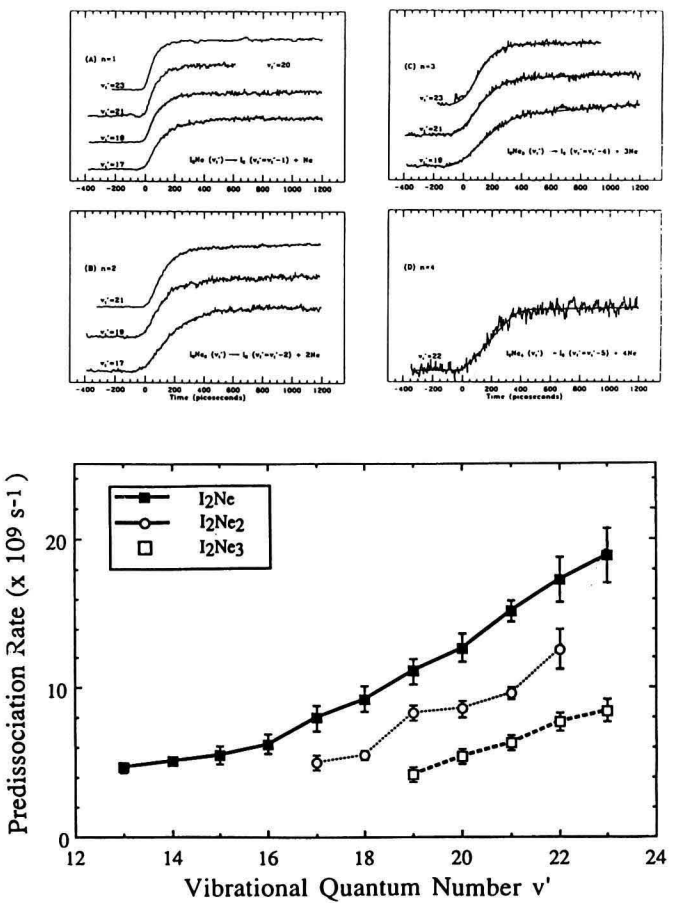

Fig. 15. The dependence of the rates on the cluster size (Ne; $n = 1, 2, 3, 4$), and on the initial vibrational quantum number [Gutmann, 1992; Gutmann, 1992].

in Fig. 15. It is useful to note that as the number of solvent atoms increases, the rates decrease. Furthermore, the 'onset' for vibrational relaxation (i.e., condensed phase effect) begins with two solvent atoms on this *picosecond* time scale (Gutmann, 1992).

Changing the rare gas atom to argon results in a new channel. In addition to evaporation, the argon causes the breakage of the chemical I-I bond. The solvent, in this case, mixes the bound state with a repulsive potential ('electronic predissociation'), producing $I + I + Ar$, in addition to the $I_2 + Ar$. We shall return to these two processes of evaporation and bond breakage when we consider the solvation effects in larger I_2/Ar_n clusters.

IV. Solvation in Large Cluster Cages

Solvation dynamics of chemical reactions in cluster cages offer a unique opportunity to examine the effect of a solvent on the elementary processes of bond breaking or bond making. The solvent may, for example, facilitate the remaking of a bond, in what has been termed the 'cage effect' (Frank, 1934), or it may behave as a 'chaperone' (Porter, 1992) with new reaction intermediates formed. With the ability to resolve the elementary femtosecond (fs) nuclear motions of reactions, it is of great interest to probe such motions in the presence of solvent shells that reach a unique quasi-condensed phase (Saenger, 1981; Jortner, 1990; Berry, 1990).

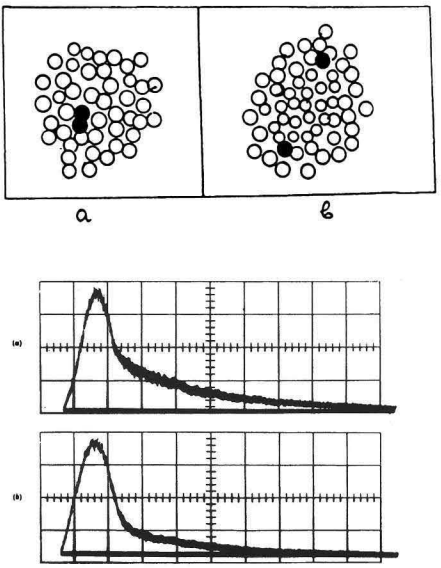

Fig. 16. Two historical figures related to iodine dissociation studies over the past 60 years. (Top) The caging idea in liquids [Frank, 1934], and (bottom) the oscilloscope traces of light output from flash lamps used in the initial flash photolysis of iodine [Porter, 1992].

In this section, we discuss studies of the real-time fs dynamics of neutral iodine dissociation and caging in clusters of argon atoms (typically 40 to 150). On this time scale, we observe the 'solvent-frozen' coherent motion of the iodine nuclei at times less that 1 ps, and the subsequent caging after the two iodine atoms are chaperoned by the argon atoms for less than 300 fs. The fs experiments give a unified picture of the mechanism which crucially depends on (i) the time scale for bond breakage and (ii) the effective temperature of the solvent. Molecular dynamics simulations are also discussed to help visualize details of the motion of the iodine solute in the argon solvent.

Direct real-time studies of clusters on the picosecond (Papanikolas, 1991; Felker, 1983; Breen, 1990; Syage, 1991; Gutmann, 1992) and femtosecond (Baumert, 1992; Potter, 1992; Papanikolas, 1992; Wei, 1992; Schreiber, 1992) timescales and molecular dynamics simulations (Amar, 1984; Alimi, 1992; Stace, 1981) have revealed the dependence of the dynamics on the solvent and on the number of solvent atoms or molecules. From the large solvent complexes to the one-atom cages formed in molecular beams, these iodine systems provide a new way for examining solvation, and help the understanding of the asymptotic bulk properties in liquids, solids, or in compressed gases/liquids. On the ps-fs time

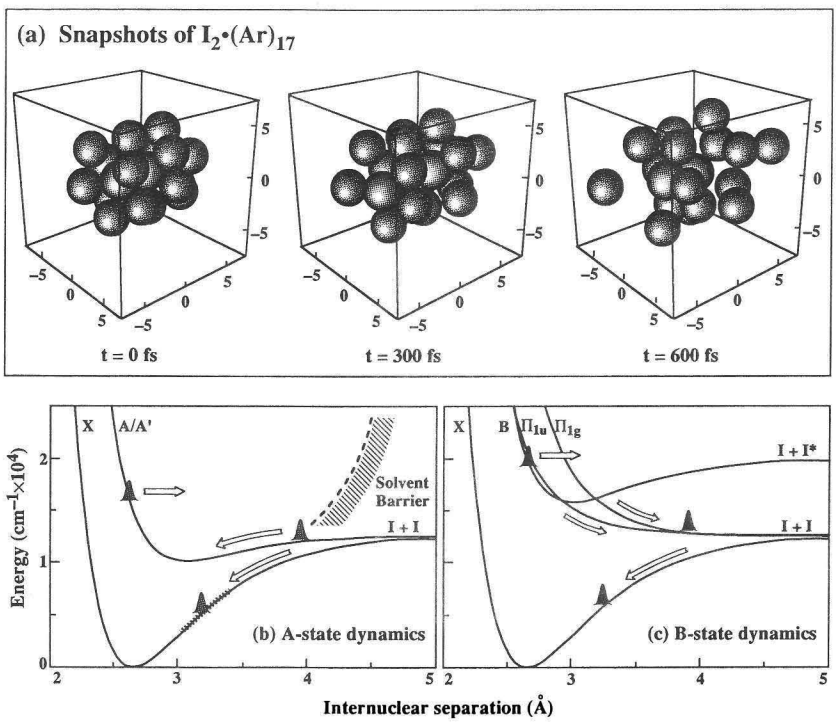

Fig. 17. (Top) Snapshots of the dynamics of iodine dissociation in argon at three times. (Bottom) The potentials describing the wave packet motion in the gas phase and in the solvent cage (schematic barrier); see Liu, 1993.

scale, the recent work in solutions (Harris, 1988; Scherer, 1992) is of great interest for comparison. Fig. 16 shows, in two cases, the earlier historical role of iodine reactions over the past 60 years.

In our experiments, the clusters of neutral iodine molecules in argon were made in a molecular beam and the femtosecond dynamics were probed following the methodology developed earlier (Khundkar, 1990; Zewail, 1988, 1993) (see Figs. 4, 5). The dissociation reaction was initiated by a femtosecond laser pulse which prepares a wave packet either on the A state above its dissociation limit (to I + I), or on the B state at different energies below or above dissociation (to I + I*). The snapshots in Fig. 17 show the deduced structures in the cluster (see below), and the relevant ground and excited state potentials (X, A/A′, B, and Π) governing the nuclear motions. A second fs pulse is used to probe (Gruebele,

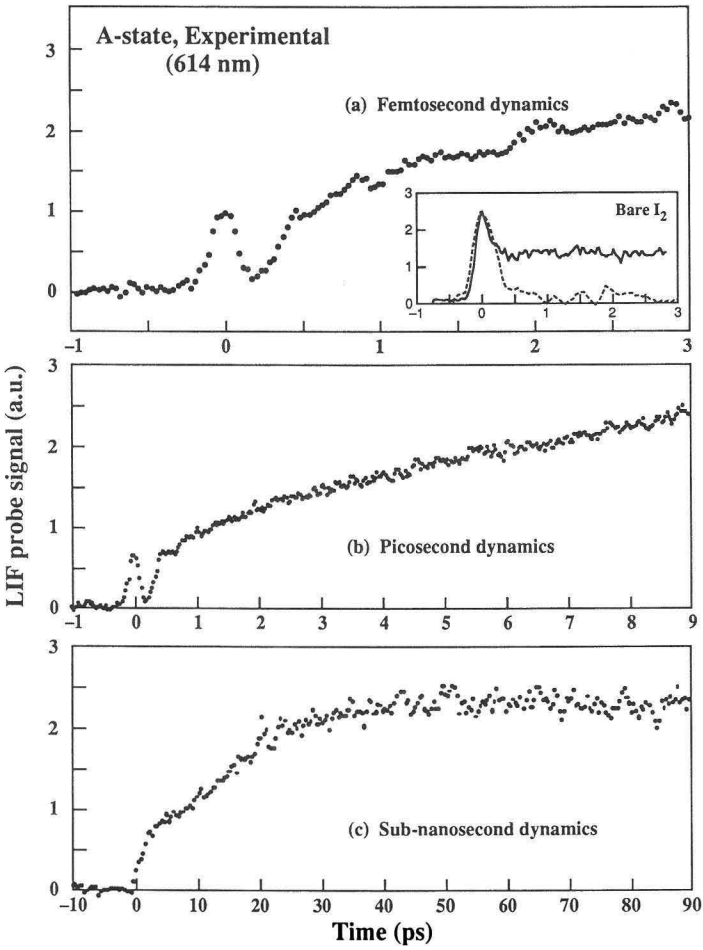

Fig. 18. Femtosecond to sub-nanosecond dynamics of iodine dissociation in argon solvent cages. The excitation is at 614 nm, and the probing is by LIF [Liu, 1993]; see text.

1993) the motion of the wave packet by detecting (Potter, 1992) the laser-induced fluorescence of I_2 in the Ar clusters at its characteristic emission (Fei, 1992). From electron diffraction, the average size of the clusters formed is estimated to range from 40 to 150 argon atoms, with an average temperature of 30 K or less. To compare the dynamics in the clusters to those of bare iodine (Gruebele, 1993), argon gas was replaced by helium which is known to form no such clusters under these expansion conditions.

Fig. 18 shows typical experimental transients obtained when iodine molecules were initially excited at 614 nm. In Fig. 18a, the first peak rise characterizes the preparation of the wave packet. The following decay reflects the fact that the wave packet is moving into a region where iodine can no longer absorb the probe pulse. In about 200 fs, the signal drops to almost zero. A fast and prompt recovery was then observed in another ~ 300 fs, which indicates that the wave packet coherently moves back to optical regions of the probe. At longer times, the signal starts to increase almost 'linearly' and much more slowly, as shown in Fig. 18b. A steady-state value is reached about 30 ps later. For the pump wavelengths ranging from 590 to 700 nm, the transients exhibit similar behaviors. The inset in Fig. 18a shows the corresponding transients obtained for the iodine-helium expansion ($\lambda_{pump} = 614$ and 640 nm), and should be compared with the behavior shown in Figs. 7 and 10.

When the pump wavelength was shorter than 590 nm (below the dissociation to $I + I^*$), the initial fs dynamics discussed above are replaced by a picosecond decay (~ 15 ps). The signal also rises again in ~ 30 ps, as shown in Fig. 19 for $\lambda_{pump} = 510$ nm. In the inset of Fig. 19 (top), a transient obtained by the same pump and probe (310 nm) is shown for the helium expansion. This transient shows the ~ 600 fs modulation which reflects the vibrational period of bare iodine molecules on the B state at this energy (Gruebele, 1993); see Figs. 7, 10. Above the B-state dissociation into $I + I^*$, we also observe the caging [Fig. 19 (bottom)], but the dynamics, as discussed below, are different.

The above results demonstrate that bare iodine (in helium expansions) behaves as expected when free of the solvent influence (Gruebele, 1993), as discussed above. In argon clusters, the motion of the wave packet is dramatically different and clearly reflects the initial coherence and the caging dynamics. To help understand details of the motion in the solvent cages, we have performed molecular-dynamics (MD) simulations. The clusters were assumed to have 17 or 44 argon atoms which form one or two argon shells about the iodine molecule (Potter, 1992). Iodine with one argon atom was also considered. A simulated transient was obtained by accumulating the time when the trajectories of the iodine molecules were within the probe windows. Fig. 20 shows the MD transients of the A-state dynamics, and those of the B-state, together with the intrinsic change in the I-I distance with time. The MD simulations reproduce essentially all major features of the experimental fs and ps transients. They also show how the bond energy, distance, and cluster temperature change with time.

The microscopic picture of the motion in the solvent cage now develops. Fundamentally, we observe the different types of motion which lead to what we

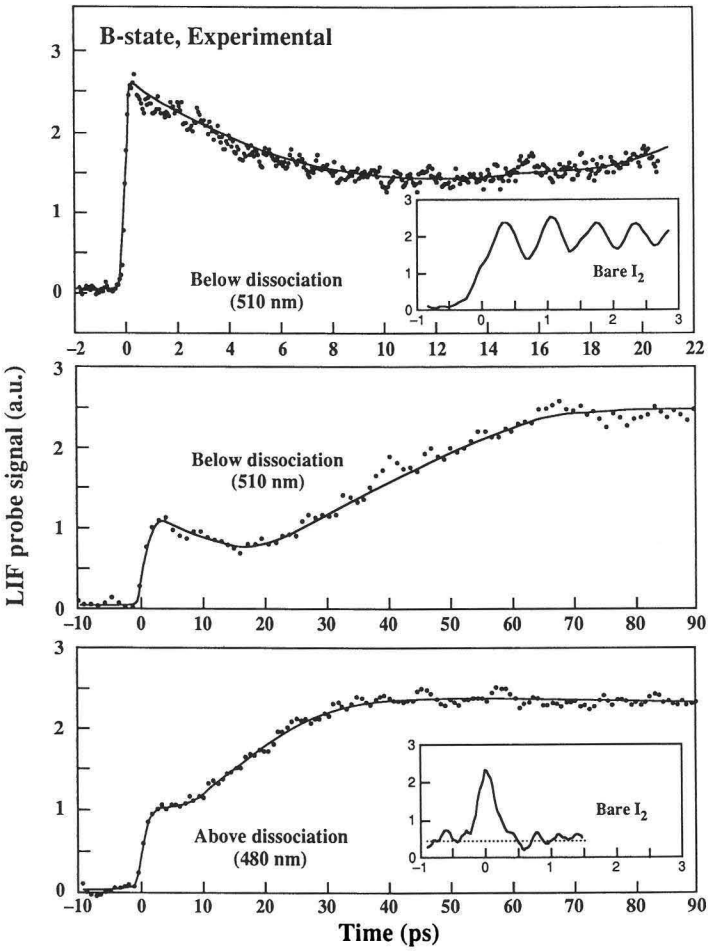

Fig. 19. The same condition as in Fig. (18), but with the initial excitation either at 510 nm (below dissociation) or at 480 nm (above dissociation). Note the contrast with the results in Fig. (18); see text.

term '*coherent*' and '*diffusive*' caging. When iodine is excited above dissociation into I + I (A-state), the wave packet moves to the region of the solvent barrier made of the repulsion with argon atoms. It then bounces back and reaches the probe window coherently and the first prompt recovery of the signal is observed (Fig. 18). On this ~ 500 fs time scale, the solvent is still 'frozen' and from the observed time delay, we estimate a solvent barrier at ~ 4.4 Å. Transferring energy to argon through periodic collisions, the iodine recombines and relaxes on the X and/or A/A′ states. If this energy release is 'non-statistical,' one expects a step-wise build-up of the signal because of the step-wise motion into more favorable regions of the probe as the I-I distance decreases towards the equi-

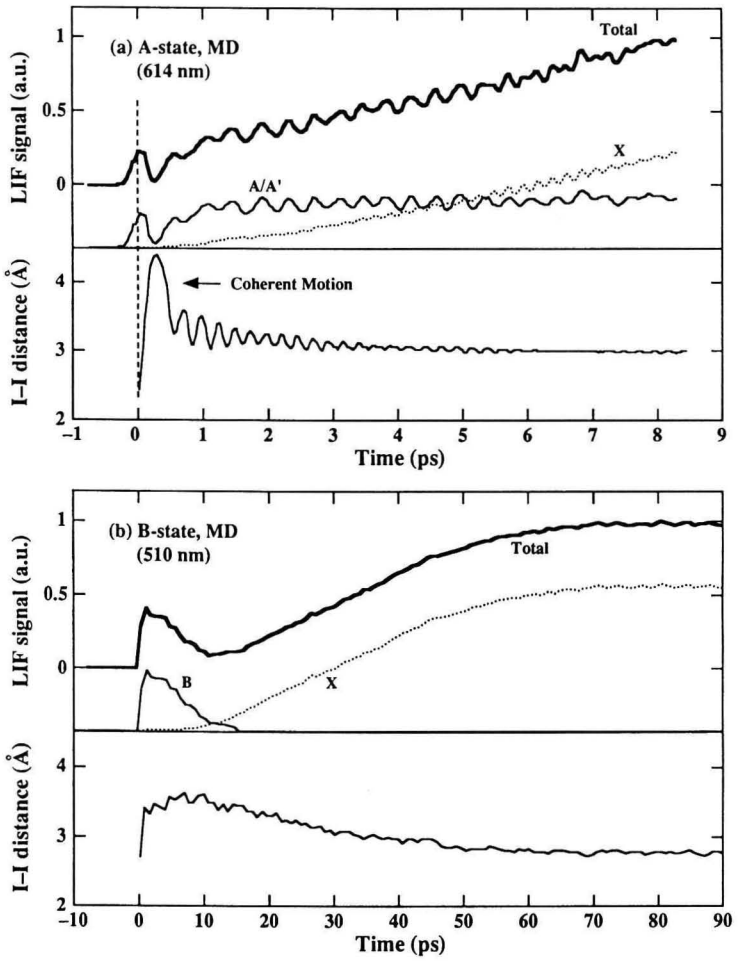

Fig. 20. Molecular dynamics (MD) simulations of A-state and the B-state type behavior. Both the LIF signal and the change in the I-I distance are displayed. (Not shown are the changes in energy, temperature and cluster size with time [Potter, 1992, and work to be published]; Liu, 1993, see text.

librium value. The slope of this linear rise depends on the cluster size, but the shape is indicative of caging.

The time scale of bond breakage is fundamental to the subsequent caging dynamics. For the A-state type dissociation (or for the repulsive states), it is typically 200-400 fs, consistent with the time scale for coherent caging. It also indicates that argon chaperone of iodine is no longer than 300 fs. Bond breakage on the quasi-bound B-state takes a much longer time. Iodine with one argon predissociates in about 70 ps (depending on the energy, see Section III) (Gutmann, 1992); and in our clusters, we observe an initial decay of ~ 15 ps instead of the coherent decay of ~ 200 fs on the A-state. The long ps B-state dynamics

allow for efficient energy transfer and for the cluster to soften its structure and the solvent barrier to decrease in energy. As supported by MD simulations, once dissociated, the two iodine atoms can be found at long internuclear distances, allowing solvent atoms to intervene between them.

The consequence of this 'diffusive' solvent motion is a longer caging time and equilibration (exponential rise; see Figs. 19, 20) in the recombination. The caging time in this case ranges from 5-10 ps (delay time for the rise); this too is evident in the theoretical simulations and in the experimental transients here and also in (Potter, 1992). The phenomenon of diffusive caging brings an analogy to liquids, where the motion of the solvent and the finite temperature could mask the coherent caging observed here. In a matrix at low-temperatures, the rigidity should allow for the observation of the direct motion (Alimi, 1992), provided the matrix phonons are not a problem for energy relaxation and dephasing of the initial packet. Work on caging of I_2 in argon matrices would be of interest, and this system is currently under study in the groups of A. Apkarian and D. Imre.

Above the B-state dissociation limit, we observe the A-state type caging, in addition to quasi-bound B-state contribution. On the B-state, above its dissociation, caging is achieved by energy transfer to argon and trapping in the bound potential, with the packet oscillation back and forth.

Future extension of this work (Liu) in this laboratory will be aimed at experimental and theoretical studies of the dynamics in the cluster phase (different compositions), as shown here, or at high pressures as reported before[3] and discussed below. Since our focus is on neutral systems, we will not be able to reach the mass-resolution of the original studies of $I_2^-(CO_2)_n$ (Papanikolas, 1992). However, our interest is in large solvation shells and the scaling laws of cluster size are quite adequate. With the help of MD in clusters and at high pressures, these studies promise a new direction for fs dynamics of solvation.

V. At the Interface to Liquids

The same systems have been studied at high pressures in order to change the 'degree of order' of the solvent around the solute. Unlike cluster cages, at high pressures there is no stacking geometry. Instead, the radial distribution function reflects the structure of the solvent shells. For iodine in argon, say at 100 atmospheres, the density of argon is about 3 atoms per nm^3, and the radial distribution function is typically that shown in Fig. 21.

The solvation effect is manifested in a number of ways depending on the total energy below dissociation in the B state, and above dissociation to $I + I^*$. In Fig. 21, the influence of this density change on the dephasing and rephasing of the isolated wave packet [Fig. 7] is shown. At three energies (see Fig. 10), the

[3] See Zewail, 1992 for work up to 100 atmospheres. For studies at higher pressures, up to 2000 atmospheres, see Lienau (1993).

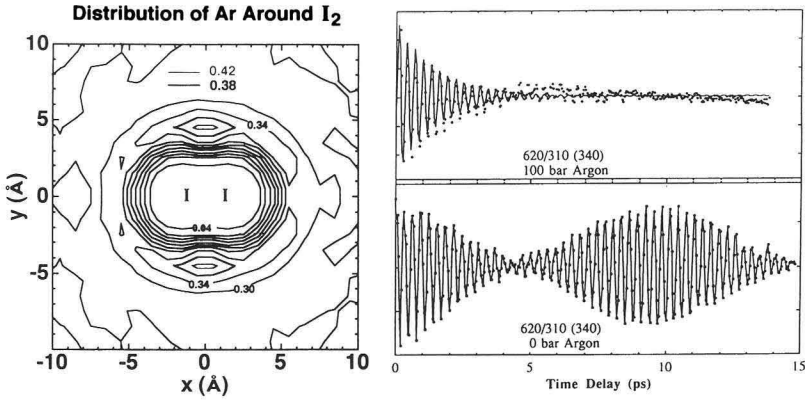

Fig. 21. (Left) The distribution of argon around iodine at 100 atmospheres of pressure. (Right) The effect of the pressure on the wave packet motion [Zewail, 1992; Yan, 1992].

behavior at 100 atmospheres is contrasted with that of 'zero pressure' (Fig. 22). Significant changes are observed. For bare iodine, we observe energy-dependent dynamics. Above dissociation, the wave packet of iodine freely moves to longer internuclear separations without return. Near dissociation, the packet returns with almost 50% probability, displaying a 'chirped-packet' behavior. Below dissociation, the wave packet returns back and oscillates between the turning points, just as described before in Fig. 10.

At high pressures, the changes are significant in showing the effect of the solu-

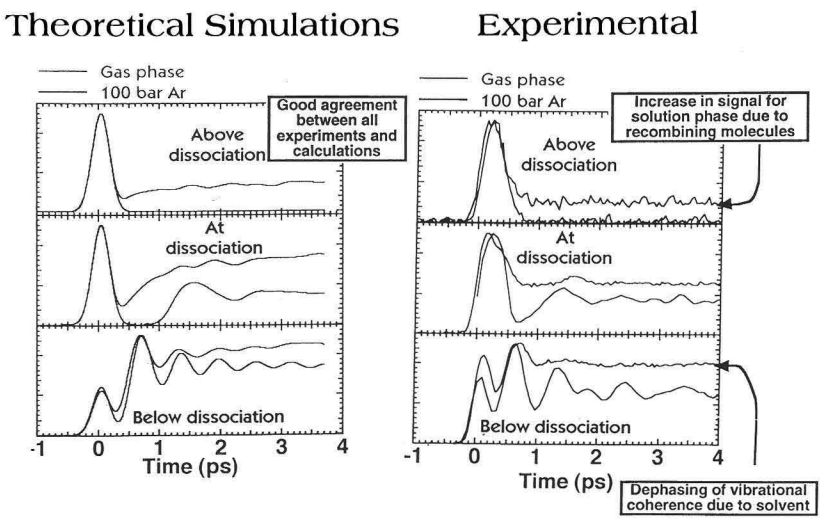

Fig. 22. Experimental and molecular dynamics studies of the wave packet motion in the gas phase and at 100 atmospheres of pressure for three energies; above, at, and below dissociation. The gas phase data are 'below' those of the high-pressure data [Zewail, 1992; Yan, 1992].

tion phase on the caging and relaxation. Unlike the cluster case, the caging observed when the I-I bond is broken above the dissociation limit shows no clear evidence of the coherent motion discussed above. This indicates the phase averaging imposed by the dynamic solvent effect at high pressures. At dissociation, there is change in the asymptotic level and one also observes changes in the nature of the oscillating motion at $t = 0$ and longer times. Below dissociation, we observe the dephasing of vibrational coherence due to the solvent (see Fig. 22).

The Wilson's group (Yan, 1992) has shown (Fig. 22) that the dynamics at high pressures can be simulated from 'ab initio' dynamical calculations. (See also Section IV.) At the three energies studied, the simulations reproduce the major features of the experiments and quantify the contributions of caging, vibrational relaxation, and dephasing on the time scale of their occurrence.

Much more work will be forthcoming in this area as we hope to examine the role of solvation at more than 100 atmospheres of pressure to compare and contrast with the cluster cage work, described above, and also with the liquid and matrix work. The apparatus for these very high pressures is now completed at Caltech and data for I_2 in argon at $\sim 2{,}000$ atmospheres have already been obtained (Lienau, 1993).

VI. Reactions and Their Control

This section describes the extension of the above studies to the xenon system, and, additionally, the use of this system to demonstrate the control of chemical reaction yield on the femtosecond time scale.

Before discussing this reaction yield control, it is useful to show the control of wave packet population with femtosecond pulses. Stimulated by earlier work on multiple and phase-coherent (ns) pulse techniques (Warren, 1983; Orlowski, 1978), we have used two fs pump pulses (instead of one) to prepare two wave packets either fully *in-phase* or *out-of-phase*. A third pulse is used to probe the motions of the two packets. This pulse sequence defines a phase angle (between the first two pulses) for a 2-D wave packet transients with $\theta = \omega_1 \tau_1$, where ω_1 is a frequency that can be made to match any of the packet frequencies (i.e., periods of motions) and τ_1 is the delay time. For a period of say 300 fs, if we use τ_1 of 150 fs, then $\theta = \pi$. Accordingly, the phase should be 180° shifted (see Fig. 23). Prepared in such a way, the two packets will then be out-of-phase and no oscillations should be observed. On the other hand, if $\theta = 4\pi$, then we should be able to double the population *in-phase*. This is reminiscent of the first observation of *in-phase* and *out-of-phase* coherence in studies of IVR by Felker et al. (Felker, 1983; Felker, 1988), but now provides an opportunity for packet population control with the phase of the motion well defined.

The experimental results (Gerdy, 1990) relating to these concepts are shown in Fig. 23, also for iodine. The results indicate that one is able to prepare two wave packets in-phase or out-of-phase with minimum spreading and a high degree of localization. We therefore should be able to use this approach to con-

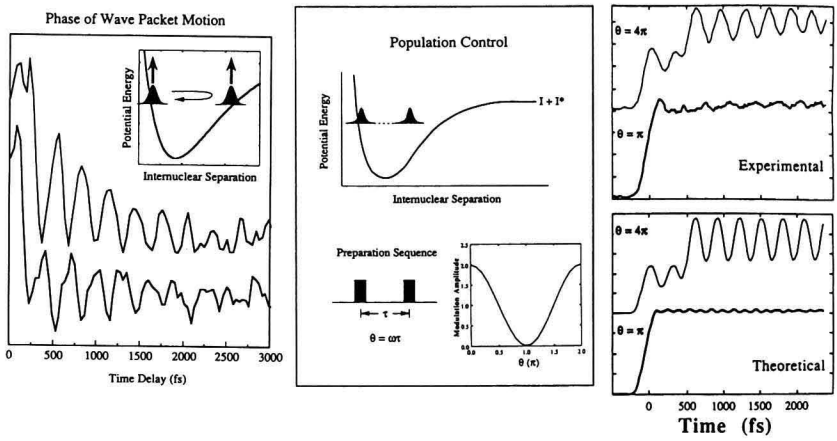

Fig. 23. Control of wave packet population in iodine using a pair of pulses for preparation and a third one for probing. (Left) The in-phase and out-of-phase motions as probed at the two turning points. (Middle) Scheme for packet transfer and phase angle (θ) control. (Right) Experimental and theoretical results [Gerdy, 1990]; see text and also [R.M. Bowman, M. Dantus, and A.H. Zewail, *Chem. Phys. Lett.* **174**, 546 (1990)].

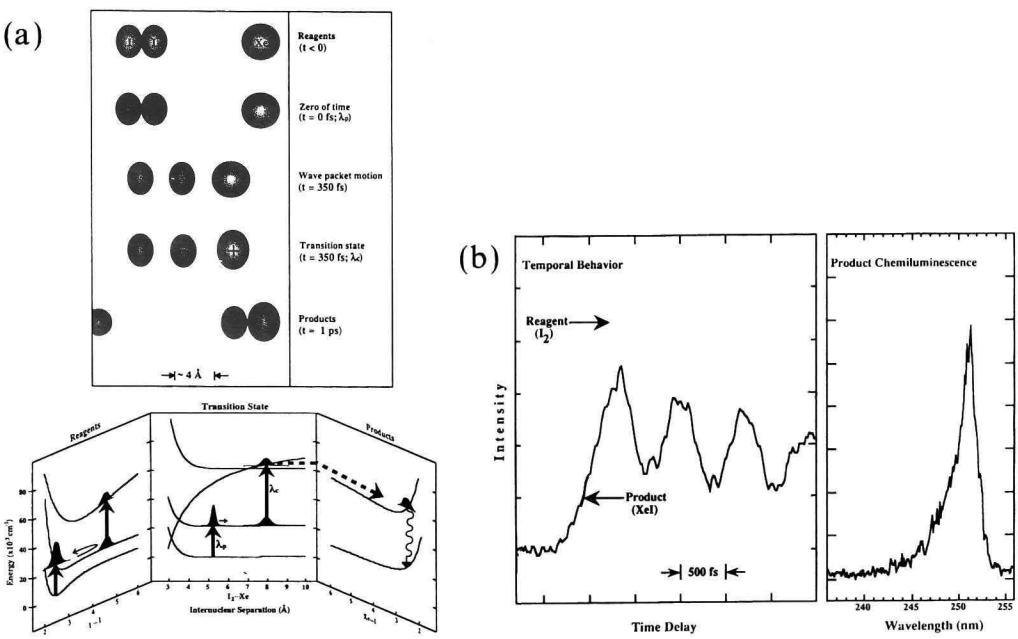

Fig. 24. Control of reaction yield with fs pulses. (a) Schematic of the motion and the potentials involved. (b) Experimental results for $I_2 + Xe$ reaction. The product yield is monitored through its chemiluminescence, which follows the 'harpoon' process. Note that the modulation of the yield of XeI follows that of the nuclear motion (Reference: E.D. Potter, J.L. Herek, S. Pedersen, Q. Liu, and A.H. Zewail, *Nature* **355**, 66 (1992)]; see text.

trol the reactivity of a chemical reaction since both the *timing* and the *phase* of the motion can be established. Recent theoretical studies by Tannor (Somloi, 1993) have explored control pathways in I_2 and further experiments should utilize this experimental approach. We have not specified the phase of the pulses as done in the earlier ns work (Warren, 1983; Orlowski, 1978), also on I_2, but the recent fs work (Scherer and Fleming) has obtained the wave packet dynamics with specified pulse phases, giving an additional feature to the control experiments on the fs time scale.

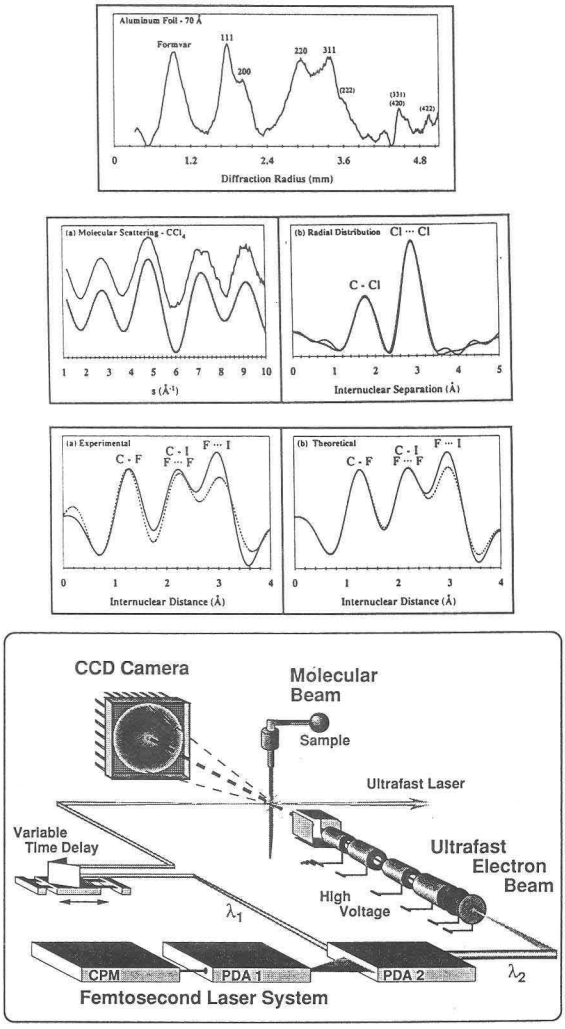

Fig. 25. Ultrafast electron diffraction. (Top) Experimental results taken for different systems (aluminum foil - 70 Å, CCl_4, CF_3I) and (bottom) the apparatus which includes a fs laser system, a CCD camera, electron optics, and the molecular beam [Williamson, 1991; 1992; 1993; 1994].

Iodine reacts with xenon to form xenon iodide with the following elementary steps:

$$Xe + I - I^* \rightarrow [Xe^+ \cdot \cdot I^- \cdot \cdot \cdot I]^{*\ddagger} \rightarrow XeI^* + I. \quad (5)$$

This reaction is a type of 'harpoon reaction' and proceeds by electron transfer in the transition-state region, Fig. 24. When iodine is excited into the B-state, the wave packet moves toward the outer turning point with the change in phase shown above. If a second (control) pulse is used, this packet can be promoted (at the critical time and with the relevant phase) to the harpoon region of the potential, thus inducing product formation. Conceptually, the idea is to exploit the timing of the motion of the packet by the two pulses and to monitor the yield of the product XeI (through its chemiluminescence). If the packet arrives at 'the right time at the right place' for the controlling pulse to promote, we should then see a yield, but if the packet is not at this particular configuration, then no yield will be observed.

Fig. 24 shows this control of the yield for the $Xe + I_2$ system with the 'period of yield modulation' following the period of the nuclear motion in the reactant I_2. (The modulation depth is $\sim 100\%$, here limited by the width of our uv pulses). It is remarkable that this effect, which we termed the 'switch effect,' clocks the bimolecular encounter and controls the outcome of the product. Naturally, we are extending these first studies to a number of systems. Studies are also planned in large and small solvent clusters in the beam to explore their relevance to the solvation of iodine (in the series He, Ne, Ar, Kr, and Xe) and for the precursor-geometry effect on bimolecular reactions (Scherer, 1990; Ionov, 1992). The mechanism of the control of the wave packet as related to the switch effect in the reactants or in the transition-state is of considerable interest to us. Theoretically, this control of the wave packet on the fs time scale has been advanced for different schemes (Tannor, 1988; Manz, 1992; Wilson, Warren, this proceeding), and more experiments will surely be forthcoming; perhaps the chemists' dream of ultimate control will be fulfilled using ultrashort laser pulses (Zewail, 1980; Bloembergen, 1984).

VII. Concluding Remarks

Studies of molecular reaction dynamics on their fundamental time scale - femtoseconds - have opened up new and exciting opportunities for understanding chemical reactions as they actually happen. Studies in femtochemistry include reactions in the gas phase/molecular beams, in clusters, on surfaces, and at the interface to the condensed phase (see Appendix I). Larger and more complex sytems have also been studied [see Zewail, 1993, 1994, and references therein]. In addition to the FTS methodology, which is the standard technique for such studies, we are also advancing the recently developed ultrafast electron diffrac-

tion method (Williamson, 1991; 1992; 1993; 1994; Dantus, 1994) (see Fig. 25) for studies of complex structures in real-time.

This article focused on the application to one elementary reaction in the isolated (gas phase/molecular beam) phase, in solvent cages, and in solutions. Some recent developments, including extensions to the control of the reaction population and yield, are also discussed.

The important contributions in this volume is a testimony to the versatility and to the diversity in the field. Studies of reactions and molecular dynamics with fs resolution are now finding significant and bread applications in Chemistry and Biology. We have reached the ultimate time scale for the nuclear motions to observe and study the elementary transition states, and to localize the motion (wave packet). The field is continuing to expand with a large community for research in both experiment and theory.

References

Alimi, R., Gerber, R.B., McCaffray, J.G., Hunz, H., Schwentner, N., *Phys. Rev. Lett.* **69**, 856, 1992.

Amar, F.G., Berne, B.J., *J. Phys. Chem.* **88**, 6720, 1984.

Baumert, T., Engle, V., Meier, C., Gerber, G., *Chem. Phys. Lett.* **200**, 488, 1992.

Beddard. G., *Rep. Prog. Phys.* **56**, 63, 1993.

Berry, R.S., *Proceedings of the International School of Physics*, ed., Scoles, G., North-Holland, Amsterdam, p. 3, 1990.

Beswick, J. A., Jortner, J., *Adv. Chem. Phys.* **47**, 363, 1981.

Breen, J.J., Peng, L.W., Willberg, D.M., Heikal, A., Cong, P., Zewail, A.H., *Chem. Phys.* **92**, 805, 1990.

Bloembergen, N., Zewail, A.H., *J. Phys. Chem.* **88**, 5459, 1984.

Dantus, M., Roberts, G., *Comments Atomic & Mol. Phys.* **26**, 131, 1991.

Dantus, M., Kim, S.B., Williamson, J.C., Zewail, A.H., *J. Phys. Chem.* **98**, 2782 (1994).

Fei, S., Zheng, X., Heaven, M., Tellinghuisen, J., *J. Chem. Phys.* **97**, 6057, 1992.

Felker, P.M., Zewail, A.H., *Chem. Phys. Lett.* **94**, 454 (1983).

Felker, P.M., Zewail, A.H., *J. Chem. Phys.* **78**, 5266 (1983).

Felker, P.M., Zewail, A.H., *Chem. Phys. Lett.* **102**, 113, 1983.

Felker, P.M., Zewail, A.H., *Adv. Chem. Phys.* **70**, 265, 1988.

Fleming, G., Scherer, N., Ziegler, L.: in this proceeding.

Frank, J., Rabinovitch, E., *Trans. Faraday Soc.* **30**, 120, 1934.

Gerdy, J., Dantus, M., Bowman, R.M., Zewail, A.H., *Chem. Phys. Lett.* **171**, 1, 1990.

Gruebele, M., Zewail, A.H., *J. Chem. Phys.* **98**, 883; and references therein, 1993.

Gutmann, M., Willberg, D.M., Zewail, A.H., *J. Chem. Phys.* **97**, 8037, 1992.

Gutmann, M., Willberg, D.M., Zewail, A.H., *J. Chem. Phys.* **97**, 8048, 1992.

Harris, A.L., Brown, J.K., Harris, C.B., *Ann. Rev. Phys. Chem.* **39**, 341, 1988.
Ionov, S.I., Brucker, G.A., Jaques, C., Valachovic, L., Wittig, C., *J. Chem. Phys.* **97**, 9486, 1992.
Jortner, J., Scharf, D., Ben-Horin, N., Even, U., Landman, U., *Proceedings of the International School of Physics*, ed., Scoles, G., North-Holland, Amsterdam, p. 43, 1990.
Khundkar, L.R., Zewail, A.H., *Ann. Rev. Phys. Chem.* **41**, 15; and references therein, 1990.
Levine, R.D., Bernstein, R.B., 'Molecular Reaction Dynamics and Chemical Reactivity,' Oxford University Press, Oxford, 1987.
Lienau, C., Williamson, J.C., Zewail, A.H., *Chem. Phys. Lett.* **213**, 289 (1993).
Liu, Q., Wang, J.-K., Zewail, A.H.: *Nature* - **364**, 427 (1993).
Manz, J., *Faraday Discuss. Chem. Soc.* **91**, 358, 1991.
Manz, J., *Chem. Phys. Lett.* **198**, 483, 1992.
Orlowski, T.E., Jones, K.E., Zewail, A.H., *J. Chem. Phys.* **54**, 197, 1978.
Papanikolas, J.M., Gord, J.R., Levinger, N.E., Ray, D., Vorsa, V., Lineberger, W.C., *J. Phys. Chem.* **95**, 8028, 1991.
Papanikolas, J.M., Vorsa, V., Nadal, M.E., Campagnola, P.J., Gord, J.R., Lineberger, W.C., *J. Chem. Phys.* **97**, 7002, 1992.
Porter, G., 'The Chemical Bond: Structure and Dynamics', ed., Zewail, A.H., Academic Press, Boston, p. 113, and references therein, 1992.
Potter, E.D., Liu, Q., Zewail, A.H., *Chem. Phys. Lett.* **200**, 605, 1992.
Saenger, K.L., McClelland, G.M., Herschbach, D.R., *J. Chem. Phys.* **85**, 333, 1981.
Scherer, N.F., Ziegler, L.D., Fleming, G.R., *J. Chem. Phys.* **96**, 5544, 1992.
Scherer, N.F., Sipes, C., Bernstein, R.B., Zewail, A.H., *J. Chem. Phys.* **92**, 5239, 1990.
Schreiber, E., Kühling, H., Kobs, K., Rutz, S., Wöste, L., ber. Bunsenges, *Phys. Chem.* **96**, 1301, 1992.
Somloi, J., Kazakov, V., Tannor, D.J., *Chem. Phys.* **172**, 85, 1993.
Stace, A.J., *J. Chem. Soc. Faraday Trans II* **77**, 2105, 1981.
Syage, J., Steadman, J., *J. Chem. Phys.* **95**, 2497, 1991.
Tannor, D.J., Rice, S.A., *Adv. Chem. Phys.* **70**, 441, 1988.
Warren, W.S., Zewail, A.H., *J. Chem. Phys.* **78**, 2298, 1983.
Wei, S., Purnell, J., Buzza, S.A., Stanley, R.J., Castleman, Jr., A.W., *J. Chem. Phys.* **97**, 9480, 1992.
Willberg, D.M., Gutmann, M., Nikitin, E.E., Zewail, A.H., *Chem. Phys. Lett.* **201**, 506, 1993.
Williamson, J.C., Zewail, A.H., *Proc. Natl. Acad. Sci.* **88**, 5021, 1991.
Williamson, J.C., Dantus, M., Kim, S.B., Zewail, A.H., *Chem. Phys. Lett.* **196**, 529, 1992.
Williamson, J.C., Zewail, A.H., *Chem. Phys. Lett.* **208**, 10, 1993.
Williamson, J.C., Zewail, A.H., *J. Phys. Chem.* **98**, 2766 (1994).
Yan, Y., Whitnell, R.M., Wilson, K.R., Zewail, A.H., *Chem. Phys. Lett.* **193**, 402, 1992.

Zewail, A.H., *Science* **242**, 1645, 1988.
Zewail, A.H., Bernstein, R.B., *Chemical & Engineering News*, p. 24–43, November 7, 1988.
Zewail, A.H., *Faraday Discuss. Chem. Soc.* **91**, 207; and references therein, 1991.
Zewail, A.H., J. Chem. Soc., *Faraday Trans.* 2 **85**, 1221, 1989.
Zewail, A.H., Dantus, M., Bowman, R.M., Mokhtari, A., *J. Photochem. Photobiol. A: Chem.* **62/3**, 301, 1992.
Zewail, A.H., *Phys. Today* **33**, 27, 1980.
Zewail, A.H., *J. Phys. Chem.* **97**, 12427 (1993).
Zewail, A.H., in Femtosecond Chemistry, J. Manz and L. Wöste (eds.) VCH Verlagsgesellschaft, Weinheim (1994).

Appendix I

SOME FEMTOCHEMISTRY RESEARCH GROUPS

(Source: Invited Speakers Program of the Berlin Conferences)*

Femtochemistry in Gases I
A. H. Zewail, S. Y. Lee, M. Shapiro, Y. Chen, R. Schinke, J. H. Glownia, G. Stock

Femtochemistry in Gases II
J. L. Knee, H. D. Meyer, R. M. Bowman, H. Köppel, C. Daniel, A. A. Stuchebrukhov

Femtochemistry in Clusters I
L. Wöste, C. Wittig, P. M. Felker, G. Gerber, J. P. Visticot, M. Gruebele, V. Engel, B. Soep

Femtochemistry in Clusters II
F. G. Amar, A. W. Castleman, R. B. Gerber, J. L. Bowman, J. A. Syage, W. C. Lineberger

Femtochemistry at Surfaces
T. F. Heinz, S. Holloway, E. Mazur, T. Uzer, J. W. Gadzuk

J. Manz

Femtochemistry from Spectroscopy
J. C. Polanyi, E. J. Heller, R. D. Levine, J. L. Kinsey, D. M. Neumark, P. R. Brooks, J. P. Simons, W. H. Miller

From Femtochemistry into New Domains
G. Porter, S. H. Lin, M. Quack

Femtochemistry from Gases to Solutions
N. P. Ernsting, N. F. Scherer, D. Imre, J. Troe, S. Ruhman, T. Elsaesser, I. H. Gersonde

Femtochemistry and Laser Control
K. R. Wilson, W. Jakubetz, P. B. Corkum, R. Kosloff, A. D. Bandrauk, D. J. Tannor, G. K. Paramonov

J. L. Kinsey

* Not including other works in the condensed phases and in biology. Other groups working in the gas phase (and not present) include those at Illinois (EE & Chemistry), Colorado, Michigan State, Free University of Amsterdam, Köln University, and Université Paul Sabatier.

Author's Address

Arthur Amos Noyes Laboratory of Chemical Physics
California Institute of Technology
Pasadena, California 91125

Contribution Number 8810 from the California Institute of Technology. This research was supported by the National Science Foundation and by the Air Force Office of Scientific Research.